Materials Chemistry and Physics 139 (2013) 100–106

Contents lists available at SciVerse ScienceDirect

Materials Chemistry and Physics

journal homepage: www.elsevier.com/locate/matchemphys

Plasmon-induced photochemical synthesis of silver triangular prisms and pentagonal bipyramids by illumination with light emitting diodes

Martín D. Bordenave [a], Alberto F. Scarpettini [a,1], María V. Roldán [b,c], Nora Pellegri [b,c], Andrea V. Bragas [a,d,*]

[a] Departamento de Física, Facultad de Ciencias Exactas y Naturales, Universidad de Buenos Aires, Pabellón 1, Ciudad Universitaria, 1428 Buenos Aires, Argentina
[b] Laboratorio de Materiales Cerámicos, FCEIyA, Universidad Nacional de Rosario, Av. Pellegrini 250, 2000 Rosario, Santa Fe, Argentina
[c] IFIR, CONICET, 27 de Febrero 210 bis, 2000 Rosario, Santa Fe, Argentina
[d] IFIBA, CONICET-UBA, Pabellón 1, Ciudad Universitaria, 1428 Buenos Aires, Argentina

HIGHLIGHTS

- Ag nanoprisms and bipyramids were grown by illuminating silver seeds with LEDs.
- The final size is always determined by the wavelength of irradiation.
- Conversion rate defines the final morphology of the nanoparticles.
- Wavelength-shift respect to the plasmon of the seeds determines morphology.

GRAPHICAL ABSTRACT

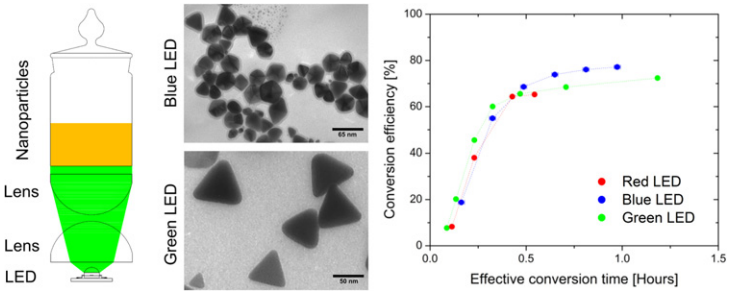

ARTICLE INFO

Article history:
Received 12 October 2012
Received in revised form
18 December 2012
Accepted 22 December 2012

Keywords:
Metals
Nanostructures
Chemical synthesis
Optical properties

ABSTRACT

We have grown silver prisms and pentagonal bipyramids, induced by plasmon excitation on a colloidal solution under the irradiation of light emitting diodes of different colors. Two methods of synthesis of the seeds were tested and their growth evolution recorded, in order to analyze the effect of the chemical synthesis and the color of the irradiation on the morphology and size of the final product. We show that the conversion rate into anisotropic nanoparticles is determined by the chemical environment and the shift of the irradiation wavelength with respect to the plasmon resonance of the seeds. The conversion rate defines the final morphology of the nanoparticles, whereas the size of the nanoparticles is univocally determined by the wavelength of irradiation, irrespective of the method to prepare the seed solution.

1. Introduction

Since the pioneering work of Jin [1], a variety of silver anisotropic nanoparticles (a-NPs) of different shapes have been fabricated *via* plasmon-induced growth, by illuminating a seed colloid solution with visible light [2–6]. Photoinduced growth methods are attractive due to the precise control that may be attained in the deposition of the metal ions on the seed surface, and, consequently, the potential control on the final morphology and size of the nanoparticles (NPs). For efficient conversion of the seeds onto the desired nanostructure, the choice of the chemical synthesis and the wavelength of irradiation are recognized as fundamental parameters. Under resonant plasmon excitation and chemical favorable environment, the spherical seed nanoparticle (s-NP) acts as a nanoreactor with well-defined and preferential sites for silver ions deposition [7–10]. It has been shown

* Corresponding author. Departamento de Física, Facultad de Ciencias Exactas y Naturales, Universidad de Buenos Aires, Int. Guiraldes 2160, Pabellón 1, Ciudad Universitaria, 1428 Buenos Aires, Argentina Tel./fax: +54 11 4576 3426.
E-mail address: bragas@df.uba.ar (A.V. Bragas).
[1] Present address: Facultad Regional Delta, Universidad Tecnológica Nacional, San Martín 1171, 2804 Campana, Buenos Aires, Argentina.

0254-0584/$ – see front matter © 2013 Elsevier B.V. All rights reserved.
http://dx.doi.org/10.1016/j.matchemphys.2012.12.061

in many works that the wavelength of irradiation controls the final size of the nanostructure [3,6,11,12]. In this work, we systematically studied the effect of the power density and illumination wavelength on the conversion efficiency, by illuminating the sample with high power light emitting diodes (LEDs). Two methods of synthesis have been tested; one uses polyvinylpyrrolidone (PVP) as stabilizer and the other uses citrate and bis-(p-sulfonatophenyl)-phenylphosphine (BSPP). Although both methods are able to produce prismatic and/or pyramidal NPs under illumination, we show that the citrate-BSPP synthesis produces much better conversion efficiency (which will be formally defined later in the text). We also show that the conversion rate of the s-NPs to a-NPs, managed by the availability of Ag^+ ions and the irradiation wavelength, determines the morphology of the final product, whereas only the wavelength defines the final size, irrespective to the chemical synthesis.

2. Materials and methods

Two chemical routes were chosen to prepare s-NPs. Preparation of PVP-protected s-NPs was initiated by dissolution of $AgNO_3$ (Merck, for analysis) and PVP (Aldrich, $M_W = 29{,}000$) in ethanol to obtain a solution 0.01 M of the salt and 0.1 M of repetition units of the polymer. In this procedure, ethanol was the solvent and principal reductant, since all reagents ($AgNO_3$ and PVP) have good solubility in ethanol, and its polarity and reductant capacity enhances the stability of the NPs against oxidation [13]. PVP was used as stabilizer and secondary reductant, since it is recognized in the literature as having an important role in the development of a-NPs (see Ref. [14] and references therein). Some authors found that the ratio of repetition units of PVP to Ag^+ ions (R) influences the yield of conversion onto a-NPs [15,16]. In previous works we studied the influence of this ratio R on the yield of conversion, by irradiating the solution with white light [17,18]. Probing R values between 1 and 20 we found that a value of R equal to 10 gives the highest yield.

For the second synthesis procedure, the s-NPs were stabilized using trisodium citrate (Sigma 99%) and BSPP (Sigma) following Jin's work [1]. Briefly, 95 ml of Milli-Q water, 1 ml of 30 mM trisodium citrate (Sigma) and 0.5 ml of 20 mM $AgNO_3$ were prepared and then 4 ml of 50 mM $NaBH_4$ (Sigma) was added. BSPP (1 ml, 5 mM) was added drop-wise, obtaining the final s-NPs colloidal suspension.

To convert s-NPs to a-NPs, the samples produced from both methods were irradiated using high-power light emitting diodes (D^+LED, 5 W), controlled by a current source. A special experimental setup was designed to have a strict control of the illumination over the entire sample, taking special care in maintaining the sample uninfluenced by environmental irradiation.

NPs characterization was carried out by transmission electron microscopy (Philips EM 301 TEM). Samples were prepared by dropping a dispersion of the particles on formvar/carbon coated copper grids. The optical characterization of colloidal suspensions was performed by extinction spectroscopy, using UV–Vis spectrophotometer Shimadzu UV-1800.

3. Results and discussion

3.1. Seed nanoparticles characterization

Light yellow colloidal suspensions were obtained with both syntheses. Fig. 1 shows the normalized extinction spectra of the silver s-NPs used as seeds for photoconversion, showing a surface plasmon band around (412 ± 1) nm for the PVP-protected NPs and (398 ± 1) nm for BSPP-protected ones, indicating the presence of s-NPs.

Statistical analysis made over TEM images and calculations on the FWHM of the extinction spectra show that both populations have a lognormal distribution with similar average radius of about 6 nm with a size dispersion of 40%. The small shift in the extinction maxima positions is due to the slightly different dielectric environments. Size effects are not responsible for these shifts. Theoretical studies show that for small NPs, below 10 nm, changes in size are only visible through changes in the FWHM of the extinction peak [19,20].

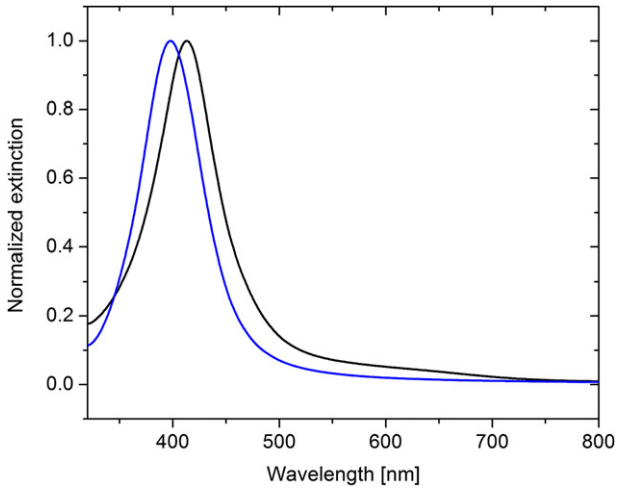

Fig. 1. Extinction spectra for spherical colloidal seeds synthesized by different methods; PVP (black) and citrate-BSPP (blue). Curves are normalized, since the difference in the extinction amplitude is only due to the different concentrations of Ag^+ ions in both syntheses. (For interpretation of the references to colour in this figure legend, the reader is referred to the web version of this article.)

3.2. Conversion efficiency

Most of the reported experiments of photoinduced growth of nanoprisms and other nano-objects in the literature are conducted by illumination with UV–visible lamps, and sometimes with lasers. The use of high-power light emitting diodes (LEDs) has several advantages over other sources of illumination. LEDs are cheap efficient electrical–optical power converters, emit in a narrow bandwidth and are suitable for collimation and guiding through an optical system. From our own experience, one of the keys for an efficient photoconversion of the NPs is to get a homogenous and power-controlled illumination of the whole container of the colloidal suspension. According to our data, power densities needed for photoconversion are around few tens of mW cm^{-2}, which is a power available for most of the high-power LEDs in the visible range. In this work we used blue: (467 ± 15) nm, green: (522 ± 15) nm, and red: (625 ± 15) nm LEDs with 5 W of nominal power.

Regarding the mechanisms responsible for photoinduced growth reported in the literature, there is evidence that for citrate-BSPP synthesis, the nearby citrate photo-oxidation due to the enhanced and localized fields under resonant plasmon excitation of the seeds produces a charge transfer to the NP and consequently a site of preferential growth, by reduction of remnant Ag^+ ions present in the solution [7] which came from a re-dissolution process of the smallest NPs (ripening Ostwald). On the other hand, it has been shown that when PVP is used as stabilizer for the synthesis of silver colloids, the polymer itself acts as an ion reductor with simultaneous oxidation of the polymer during the process [16]. The storage of a great amount of negative charges due to the free radicals reactions in the surface of the NP could be acting as the driving force for deposition of the ions on the surface [16], although the role of the light in the photoinduced growth is unknown in this case.

Fig. 2 shows the time evolution of the extinction spectra for the PVP and the citrate-BSPP colloidal synthesis illuminated with blue light, with a power density of (64 ± 3) mW cm^{-2} and (51 ± 3) mW cm^{-2}

respectively. In both cases the spectra show mainly two peaks, one around 400 nm assigned to the dipolar plasmon resonance of the s-NPs and the other one around 500 nm corresponding to a dipolar plasmon resonance for the a-NPs [1]. The additional peak around 300 nm, assigned to the out-of plane quadrupole [11], contributes to confirm the presence of a-NPs but it will not be considered in our further quantitative analysis, because of its low intensity. As time passes, the s-NPs plasmon resonance decreases at the expense of the a-NPs resonance increase, following the formation of the a-NPs [21].

Assuming that the value of the extinction for each peak is proportional to the number of s-NPs and a-NPs present in the solution at a given time respectively, we define the conversion efficiency into anisotropic particles as:

$$\varepsilon(t) = 100\frac{M_{\mathrm{a-NPs}}}{M_{\mathrm{a-NPs}} + M_{\mathrm{s-NPs}}} \quad (1)$$

where $M_{\mathrm{s\text{-}NPs}}$ and $M_{\mathrm{a\text{-}NPs}}$ are the extinction peak value for the spherical and anisotropic NPs plasmon resonances, respectively. Values in equation (1) are obtained by Lorentzian fits over the peaks of the extinction spectra.

Fig. 3 shows the conversion efficiency obtained for the two syntheses of the s-NPs seeds when are illuminated with blue light (467 ± 15) nm. Note that the conversion efficiency for the PVP synthesis is four times worse than the citrate-BSPP one. Besides, the conversion rate $d\varepsilon/dt$, during the time range for the total conversion to a-NPs, is two orders of magnitude slower. The delay observed in the formation of a-NPs for PVP, is accompanied with the growth of the s-NPs plasmon (Fig. 2(b)), revealing that there was a previous photoconversion of the Ag^+ ions in s-NPs before the conversion into the a-NPs.

3.3. Power dependence

Results of the conversion efficiency for the irradiation with blue light for citrate-BSPP synthesis at three different power densities are shown in Fig. 4. First, we observe that by irradiation with (16 ± 1) mW cm^{-2} the solution becomes unstable and collapses before concluding the whole conversion process, which is, in addition, intrinsically slow. However, for (32 ± 3) mW cm^{-2} and the double of this power (64 ± 3) mW cm^{-2}, the same saturation efficiency is reached after few hours. Although the higher power density irradiation produces a slightly faster growth, both are in the same order. It seems that once a given power density is reached in order to keep the solution stable, the power density does not affect appreciably the conversion rate.

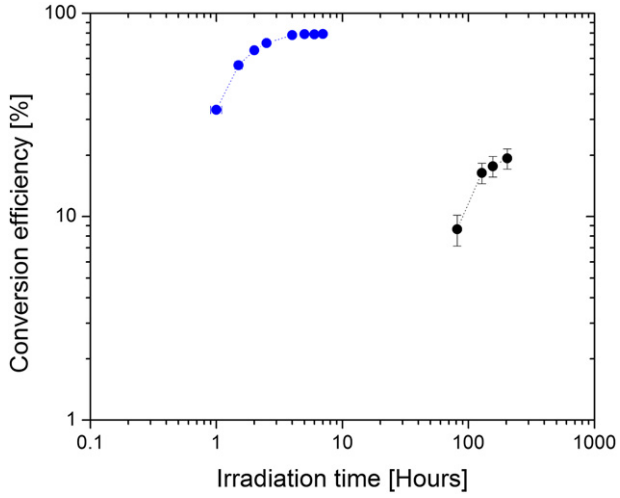

Fig. 3. Conversion efficiency (see text) of a-NPs as a function of the irradiation time for NPs stabilized with citrate-BSPP (blue) and PVP (black). The irradiation wavelength is (467 ± 15) nm. (For interpretation of the references to colour in this figure legend, the reader is referred to the web version of this article.)

Absorption of light by the NPs rise the local temperature of the solution and, since temperature has been recognized as a key factor in the final size and morphology for other silver nanoparticle synthesis [22], we tested the influence of heating in the conversion process. We heated the solutions for several hours and increased the temperature from 30 to 60 °C. We did not observe any conversion in the solution during the time of this experiment. If the temperature played a role in the conversion rate, those processes would be much slower than the photoconversion and consequently we did not take them into account.

3.4. Conversion rate and shape of the nanoparticles

The final product when the asymptote in Fig. 4 is reached has been analyzed by TEM images as the one shown in Fig. 5. We have performed a size statistics over about 200 particles using the TEM

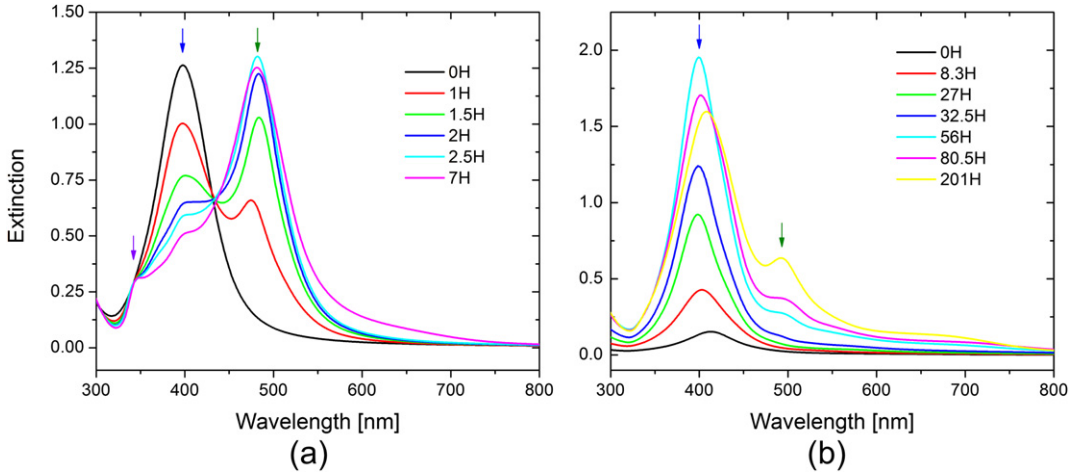

Fig. 2. Temporal evolution of the extinction spectra for the irradiation of NPs with the blue (467 nm) LED (a) stabilized with citrate-BSPP for a power density of (64 ± 3) mW cm^{-2} (b) stabilized with PVP for a power density of (51 ± 3) mW cm^{-2}. Arrows indicate the position of the plasmon resonance of spherical NPs (blue, around 400 nm), in-plane dipole resonance of anisotropic NPs (green, around 500 nm) and out of plane quadrupole resonance of anisotropic NPs (violet, around 300 nm). (For interpretation of the references to colour in this figure legend, the reader is referred to the web version of this article.)

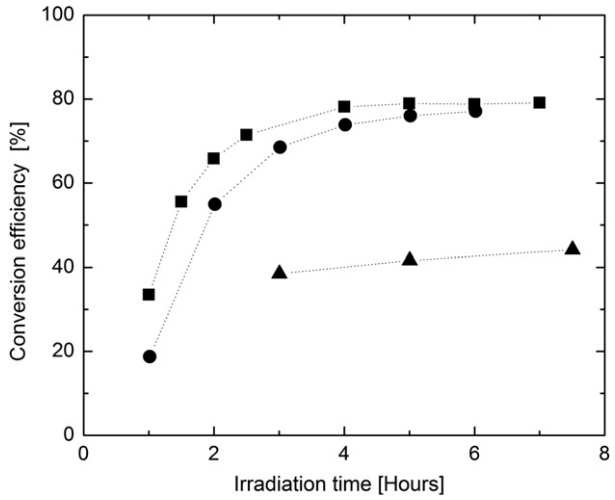

Fig. 4. Conversion efficiency of a-NPs as a function of the irradiation time for a blue LED with different power densities for the citrate-BSPP synthesis; (64 ± 3) mW cm^{-2} (square), (32 ± 3) mW cm^{-2} (circle) and (16 ± 1) mW cm^{-2} (triangle).

images, and we have obtained the mean and standard deviation from the size histograms. There are two different morphologies in the final population: 40% of triangular truncated prisms and 60% of pentagonal bipyramids. This behavior has only been observed for the sample irradiated with blue light, while for the other colors, with exactly the same initial solution and conditions, only prisms are present. The average edge is (23 ± 7) nm for the prisms and (25 ± 3) nm for the bipyramids, revealing that although the morphologies are different the final size for both objects is the same.

In Ref. [5] the authors state that modulating the rate of deposition of the silver ions on the particle surface, different morphologies of NPs can be obtained. Following the ideas of that work, we can say that a decrease of the rate of deposition leads to a preferential [100] face growth, giving rise to high aspect-ratio particles. Conversely, a higher rate of deposition, leads to a preferential growth on the [111] faces, and thus the formation of bulkier particles.

Fig. 6 shows the time evolution of the extinction curves during the irradiation of the citrate-BSPP seeds, for the three colors used. At all the irradiation wavelengths, from blue to red, the seed dipolar plasmon decreases, while the conversion into a-NPs is revealed by the growth of the in-plane dipole plasmon peak. The latter resonance shifts to the red as the irradiation wavelength increases. Additionally, the conversion rate is dictated by the wavelength of the light, as can be seen from Fig. 6(d). It decreases when the irradiation wavelength moves to the red. Therefore, and in concordance with Ref. [5], modulation of the conversion rate produces the formation of prisms at lower rates (higher wavelengths), whereas a dual-shaped distribution (bipyramids and prisms) at higher rates (lower wavelengths).

In the work of Ref. [23] the authors show different morphologies in the final product, only moving the irradiation color, but they do not give an accurate explanation of what is the reason for this apparent wavelength control on the shape of the particles. On the other hand, growth of silver nanorods by LED illumination is presented in Ref. [6]. They clearly point out that, as the excitation wavelength is further away from the plasmon resonance of the spherical seed particles, the photoreaction is slower and more controllable. This fact produces deposition only onto the tips of the particles and forms nanorods when the irradiation goes from 600 nm to 750 nm. Therefore, we can conclude, in coincidence with Ref. [6], that the conversion rate, which is directly related with the irradiation wavelength, is the parameter that dictates the final morphology of the product.

Using the data in Figs. 1 and 6(d), we calculate an effective conversion time t_{eff} as the real irradiation time, t, scaled by the extinction amplitude at the irradiation wavelength M_λ normalized to the extinction amplitude at the s-NPs plasmon resonance,

$$t_{\text{eff}} = \frac{M_\lambda}{M_{\text{s-NPs}}} t \tag{2}$$

This normalization shows that the conversion rate only depends on how far is the excitation from the seed plasmon resonance, at the same chemical environment (citrate-BSPP synthesis). Effectively, Fig. 7 shows that these effective conversion times are similar for all irradiation wavelengths.

Hence, in summary, the morphology can be controlled by the chemistry of the solution which manages the availability of Ag^+ ions and/or by the illumination wavelength.

3.5. Size of the nanoparticles

In this section we show how the illumination wavelength controls the final size of the structure. In order to check the last assumption we irradiated the seed solution obtained with the two different syntheses (PVP and citrate-BSPP s-NPs), with several different wavelengths using both LED and laser light sources. The red shift of the in-plane dipolar resonance as the irradiation

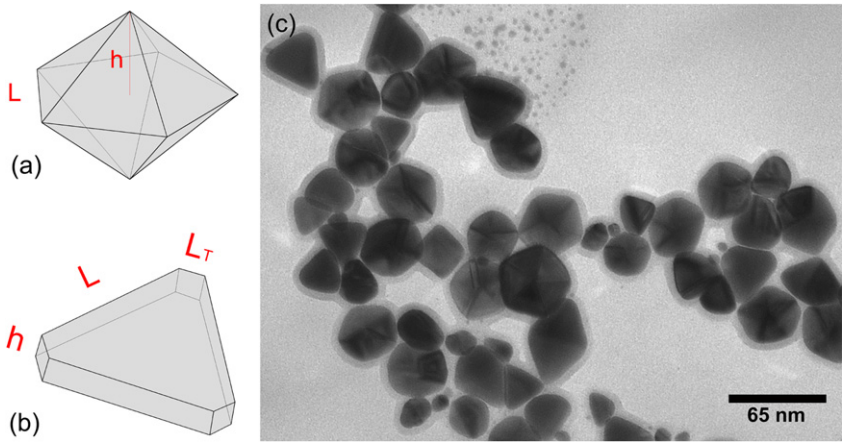

Fig. 5. Anisotropic morphologies obtained for illumination of the citrate-BSPP solution with a blue LED, power: (64 ± 3) mW cm^{-2}. Schematic representation of (a) pentagonal bipyramids and (b) truncated triangular prisms. (c) TEM image. (For interpretation of the references to colour in this figure legend, the reader is referred to the web version of this article.)

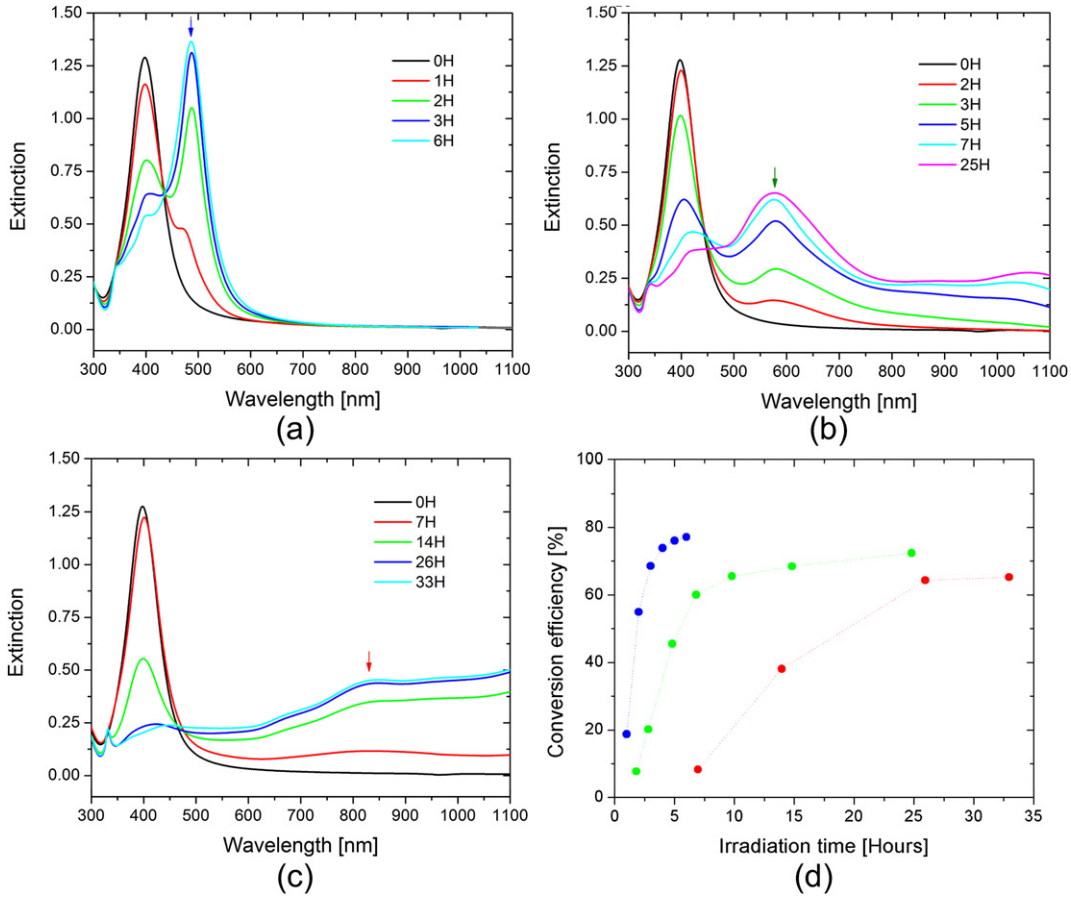

Fig. 6. Temporal evolution of the extinction spectra for the irradiation of NPs stabilized with citrate-BSPP with a (a) (32 ± 3) mW cm^{-2} of blue, (b) (32 ± 3) mW cm^{-2} of green and (c) (56 ± 3) mW cm^{-2} of red LED. Arrows indicate the position of the in-plane dipole resonance of a-NPs. (d) Conversion efficiency of a-NPs as a function of the irradiation time for a blue (blue), green (green) and red (red) LEDs. (For interpretation of the references to colour in this figure legend, the reader is referred to the web version of this article.)

wavelength increases, shown in Fig. 6 for NPs stabilized with citrate-BSPP, is associated to an NP of bigger size.

Fig. 8 shows the results of the irradiation for the two types of s-NPs. By looking at the wavelength of the a-NPs plasmon (in-plane dipolar resonance) as a function of the wavelength of irradiation, we clearly see that it follows a linear dependence, irrespective of the method of synthesis of the seed solution. This demonstrates that the chemical environment or the conversion rate is not relevant to determine the size of the final product, intimately related with the plasmon resonance position.

Fig. 9 shows TEM images of the final product for irradiation with green and red LEDs. The sizes of the obtained particles, for the three irradiation colors, are analyzed over all the TEM images and summarized in Table 1. We were not able to get the width of the prisms from our images. However, the lateral size obtained by inspection in this work is in agreement with the calculations in Ref. [24] for prisms of about 13 nm of width, which is also close to the value reported in Ref. [1]. We observe that the mean values of the characteristic lengths of the a-NPs increases with the irradiation wavelength, and it is noticeable a huge size increment for red irradiated ones.

Thus, silver a-NPs, as a mix of triangular prisms and pentagonal bipyramids, were obtained in a technique with two steps. The first step was the colloidal synthesis of the spherical seeds protected by different stabilizers: PVP and citrate-BSPP. PVP is a polymeric stabilizer [25] that binds to the silver NPs through an ion–dipole interaction. So, it forms a steric barrier to the particle growth that controls the shape because of the preferential adsorption of the polymer on different silver crystalline planes. On the other hand, citrate behaves as an ionic stabilizer [9] while the main role of BSPP is probably involved in the Ag^{+} stabilizing. The strong ion–ion interaction may be advantageous to the anisotropic growth for the citrate-BSPP technique comparatively to the PVP-assisted one

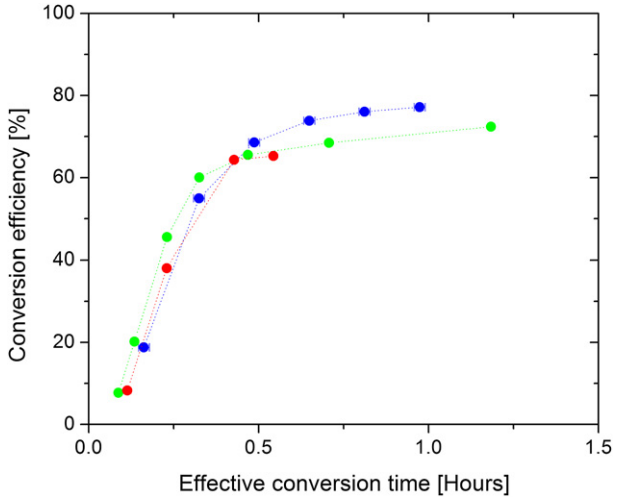

Fig. 7. Conversion efficiency of a-NPs as function of the effective conversion time for a blue (blue), green (green) and red (red) LED illumination. All the three curves have very similar characteristic times, indicating that the conversion rate depends mainly on how far is the excitation from the plasmon resonance of the seeds. (For interpretation of the references to colour in this figure legend, the reader is referred to the web version of this article.)

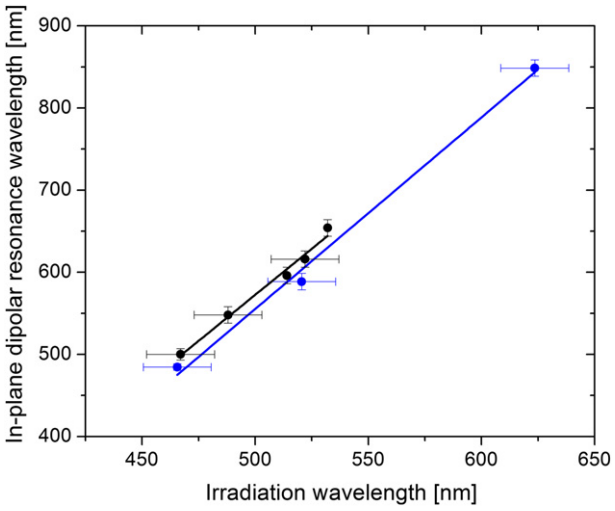

Fig. 8. In-plane dipolar resonance wavelength as a function of the irradiation wavelength for irradiation of colloids stabilized with PVP (black) and citrate-BSPP (blue). (For interpretation of the references to colour in this figure legend, the reader is referred to the web version of this article.)

in which the stabilizer binding is weaker as was suggested by Xue et al. [26]. After the step of seeds formation, spherical NPs of 6 nm were obtained while some Ag^+ ions remained unreduced in the solution of PVP protected s-NPs. In both cases (PVP and citrate-BSPP), also, the radii of the NPs were small enough to allow the re-dissolution of the smallest ones in an Ostwald ripening process. So, these are the sources of Ag^+ available to the second step which consisted of the photoinduced growth of a-NPs. When the s-NPs are irradiated with LEDs, an anisotropic distribution of charges is produced that create preferential sites for ions deposition [26] and so the asymmetrical growth is initiated.

4. Summary and conclusions

As a conclusion, we grew asymmetric NPs by irradiation with light emitting diodes of different colors a solution of silver spherical seeds colloids. We worked with two different methods of synthesis using PVP and BSPP, in order to separate the effect of the wavelength and the chemical environment in the determination of the size and morphology of the particles. We demonstrated that the final size of the NPs is univocally determined by the wavelength of irradiation, irrespective of the method to prepare the seed solution. On the other hand, a combination of the chemistry of the seed solution and the wavelength of irradiation determines the rate of photoconversion and, consequently, the morphology of the final product.

Table 1
Mean values for the lateral size, L, of the a-NPs fabricated. $\lambda_{Irradiation}$ is the wavelength of irradiation, L_T is the truncated side of the prisms and $L_{Bipyramids}$ is the lateral size of the bipyramids (see diagrams in Fig. 5(a) and (b)).

$\lambda_{Irradiation}$ [nm]	L [nm]	L_T [nm]	$L_{Bipyramids}$ [nm]
467 ± 15	23 ± 7	8 ± 3	25 ± 3
522 ± 15	32 ± 18	7 ± 4	–
625 ± 15	279 ± 89	44 ± 24	–

Acknowledgments

We would like to acknowledge Facundo Delfino and Fernando Yapur for their help with LED electronics. This work is supported by ANPCYT (PICT 2010-00825), UBA, Programación Científica 2010-2012 (Proyecto No. 20020100100719) and CONICET (PIP N° 2195/09).

References

[1] R. Jin, Y. Cao, C.A. Mirkin, K.L. Kelly, Science 294 (2001) 1901–1903.
[2] A. Callegari, D. Tonti, M. Chergui, Nano Lett. 3 (2003) 1565–1568.
[3] V. Bastys, I. Pastoriza-Santos, B. Rodriguez-Gonzalez, R. Vaisnoras, L.M. Liz-Marzan, Adv. Funct. Mater. 16 (2006) 766–773.
[4] A.M. Junior, H.P.M. de Oliveira, M.H. Gehlen, Photochem. Photobiol. Sci. 2 (2003) 921–925.
[5] J. Zhang, M.R. Langille, C.A. Mirkin, J. Am. Chem. Soc. 132 (2010) 12502–12510.
[6] J. Zhang, M.R. Langille, C.A. Mirkin, Nano Lett. 11 (2011) 2495–2498.
[7] P.L. Redmond, X. Wu, L. Brus, J. Phys. Chem. C 111 (2007) 8942–8947.
[8] P.L. Redmond, L.E. Brus, J. Phys. Chem. C 111 (2007) 14849–14854.
[9] M. Maillard, P. Huang, L. Brus, Nano Lett. 3 (2003) 1611–1615.
[10] X.M. Wu, P.L. Redmond, H.T. Liu, Y.H. Chen, M. Steigerwald, L. Brus, J. Am. Chem. Soc. 130 (2008) 9500–9506.
[11] R. Jin, Y.C. Cao, E. Hao, G.S. Métraux, G.C. Schatz, C.A. Mirkin, Nature 425 (2003) 487–490.
[12] X. Zheng, W. Xu, C. Corredor, S.P. Xu, J. An, B. Zhao, J.R. Lombardi, J. Phys. Chem. C 111 (2007) 14962–14967.
[13] I. Pastoriza Santos, L.M. Liz-Marzán, Langmuir 18 (2002) 2888–2894.
[14] I. Pastoriza-Santos, L. Liz-Marzán, J. Mater. Chem. 18 (2008) 1713–1820.
[15] T.C. Deivaraj, N.L. Lala, J.Y. Lee, J. Colloid Interface Sci. 289 (2005) 402–409.
[16] C. Hoppe, M. Lazzari, I. Pardinas-Blanco, M. López-Quintela, Langmuir 22 (2006) 7027–7034.
[17] M.V. Roldán, H. Troiani, M. Granada, O. de Sanctis, N. Pellegri, Acta Microsc. 18 (Suppl. C) (2009) 83–84.
[18] M.V. Roldán, H. Troiani, M. Granada, O. de Sanctus, N. Pellegri, Anales de la Asociación Física Argentina 20 (2008) 166–170.http://www.unicen.edu.ar/crecic/analesafa/vol20/v2034-166-170.pdf.
[19] G. Shinca, L. Scaffardi, Nanotechnology 19 (2008) 495712–495719.

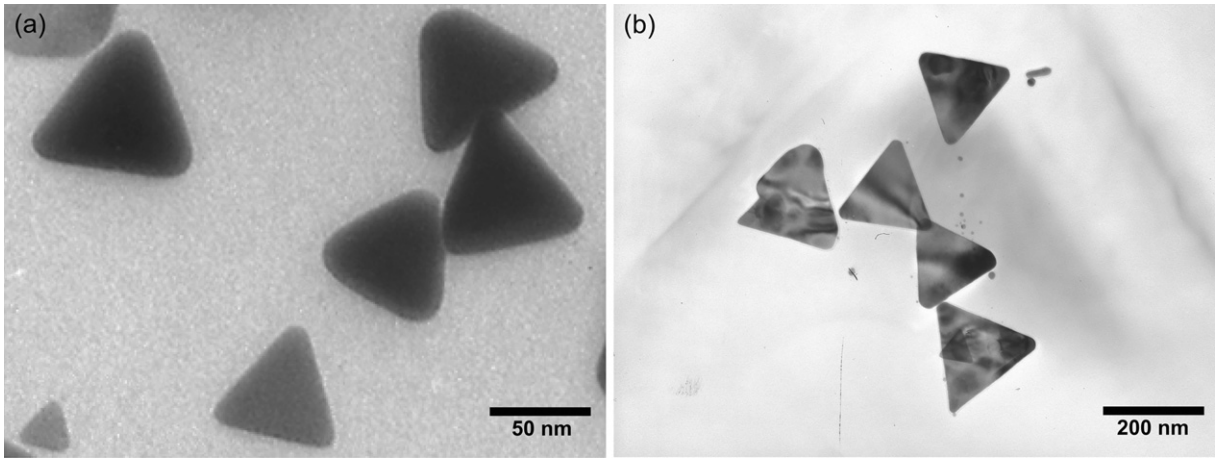

Fig. 9. TEM images of the a-NPs obtained for illumination of the citrate-BSPP solution with a (a) green and a (b) red LED.

[20] M.V. Roldán, L. Scaffardi, O. de Sanctis, N. Pellegri, Mat. Chem. Phys. 112 (2008) 984–990.
[21] The initial increase of the plasmon resonance extinction peak at 400 nm in Fig. 2(b) is attributed to the formation of spherical silver NPs from Ag^+ ions that did not react previously. This hypothesis is reinforced by the shift of the maximum extinction peak to the blue. It is known that Ag^+ ions in colloidal silver NPs may be absorbed at the surface of the NPs, to result in a change in their electronic density. This fact shifts the plasmon absorption band to blue when Ag^+ concentration decrease. Thus, the plasmon shift is indicating the decrease in Ag^+ concentration that is reduced to form metallic NPs. After 56 h of reaction a decrease of the extinction peak of s-NPs is observed, indicating that the s-NPs concentration decreases. Simultaneously, a shift of the maximum to red is observed due the formation of bigger NPs while an additional peak appears at longer wavelength that may be attributed to the in-plane dipolar absorption. All this evidence indicates the growth of a-NPs from the s-NPs.
[22] B.V. Parakhonskiy, M.F. Bedard, T.V. Bukreeva, G.B. Sukhorukov, H. Möhwald, A.G. Skirtach, J. Phys. Chem. C 114 (2010) 1996–2002.
[23] K.G. Stamplecoskie, J.C. Scaiano, J. Am. Chem. Soc. 132 (2010) 1825–1827.
[24] P. Yang, M.P. Pileni, J. Phys. Chem. C 113 (2009) 11597–11604.
[25] I. Medina-Ramireza, S. Bashirb, Z. Luoc, J.L. Liuc, Colloids Surf. B Biointerf. 73 (2009) 185–191.
[26] C. Xue, G.S. Métraux, J.E. Millstone, C.A. Mirkin, J. Am. Chem. Soc. 130 (2008) 8337–8344.